Imaging habitable planets in optical/NIR with large ground-based telescopes: WFS/C challenges, opportunities and R&D activities

Olivier Guyon[a,b,c], Mark Chun[d], Damien Gratadour[e,f], Michael Fitzgerald[g], Nemanja Jovanovic[h], Julien Lozi[c], Jared Males[b], Frantz Martinache[i], Dimitri Mawet[h], Benjamin Mazin[j], Ananya Sahoo[c], Arnaud Sevin[e], Andy Skemer[k], and Sebastien Vievard[c]

[a]Astrobiology Center; National Institutes of Natural Sciences, Tokyo, JAPAN
[b]Steward Observatory, University of Arizona, Tucson, AZ 85721, USA
[c]National Astronomical Observatory of Japan, Subaru Telescope, National Institutes of Natural Sciences, Hilo, HI 96720, USA
[d]Institute for Astronomy, University of Hawaii, Hilo, HI 96720, USA
[e]Observatoire de Paris, FRANCE
[f]Australian National University, AUSTRALIA
[g]University of California Los Angeles, USA
[h]Caltech, USA
[i]Observatoire de la cote d'Azur, FRANCE
[j]University of California Santa Barbara, USA
[k]University of California Santa Cruz, USA

ABSTRACT

Large ground-based telescopes (ELT, TMT, GMT) will have the angular resolution and sensitivity to image and characterize (spectroscopy) rocky planets in the habitable zones of nearby stars. The nearest M-type stars are particularly attractive targets thanks to moderate reflected light contrast levels and a large number of potential targets. Wavefront control and residual starlight calibration are the most significant challenges to be addressed, requiring performance levels beyond what current on-sky AO systems deliver. Extreme-AO systems will need to deliver 1e5 raw contrast within a few diffractive limits from the optical axis to allow for direct imaging of habitable planets. Differential detection techniques relying on spectroscopy, polarization and/or coherence will then be employed to separate planet signal from speckle noise. We describe technical solutions to meet the ExAO demands for direct imaging of habitable planets with ELTs.

Keywords: Exoplanets, High Contrast Imaging, Adaptive Optics, Coronagraphy

1. INTRODUCTION

1.1 Scientific background

Indirect exoplanet detection techniques (transit photometry and radial velocity) have revealed that exoplanets are abundant, and that a large fraction of stars host rocky planets in their habitable zones. Such planets have the potential to sustain liquid water and biological activity; they are referred to as potentially habitable.

Indirect detection techniques provide planet mass, orbit and radius measurements. While transit spectroscopy can also reveal atmosphere composition, most nearby habitable planets do not transit their stars, and detailed atmospheric characterization will require direct imaging to separate planet light from starlight. The upcoming generation of 25-m to 40-m ground-based extremely large telescopes (ELTs) will provide the first opportunity to

Further author information: (Send correspondence to O.G.)
O.G.: E-mail: oliv.guyon@gmail.com, Telephone: 1 818 293 8826

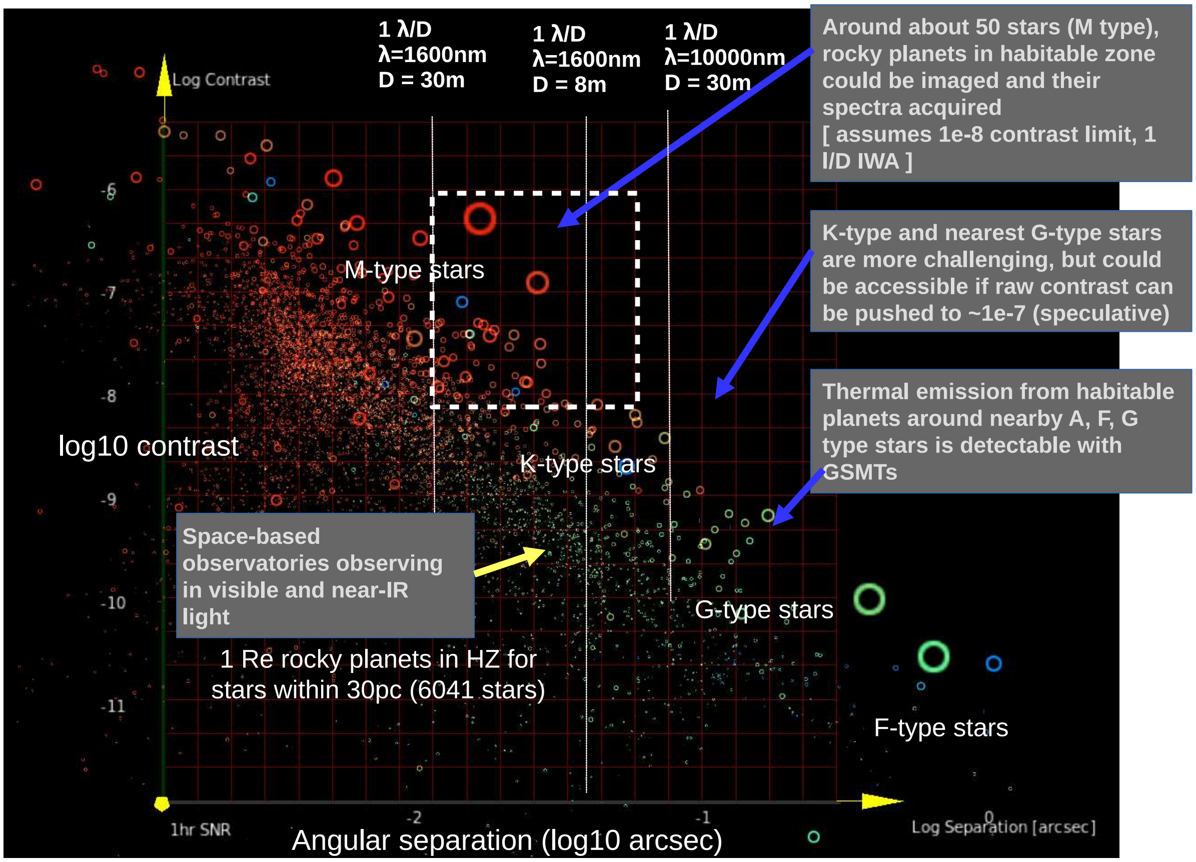

Figure 1. Angular separation (x-axis) and contrast (y-axis) of hypothetical Earth analogs around each star within 30pc. Habitable planets orbiting sun-like stars cannot be detected in reflected light from ground telescopes due to extreme contrast levels (≈ 1e-10), but they are accessible with ELTs around M-type stars thanks to more moderate contrasts.

perform the spectroscopic measurements thanks to their angular resolution and sensitivity. Near-IR spectroscopy of habitable planets orbiting nearby M-type stars appears particularly promising, thanks to moderate reflected light contrast (≈ 1e8), suitable targets, and adequate molecular absorption lines.

1.2 Exoplanet sample

We focus in this paper on the reflected light observations, where starlight reflected by the planet's atmosphere and/or surface is captured by imaging camera(s) and spectrograph(s). Thermal imaging[1] in the 5 to 13 μm spectral range, where the blackbody emission of a temperate planet peaks, is not discussed in this paper. Figure 1 shows, for each star within 30pc, the angular separation and reflected light contrast values for a hypothetical Earth-sized planet in the habitable zone of the star. The dashed rectangle indicates targets that fall within the foreseen measurement capabilities of ELTs, with contrast brighter than 10^{-8} and angular separation wider than 1 λ/D at $\lambda = 1.6\mu m$.

1.3 Instrument Design Considerations

To image and characterize exoplanets, a high contrast instrument must include the following three key functions:

- **Starlight Suppression**. A coronagraph is deployed to optically suppress starlight while maintaining high exoplanet throughput.
- **Extreme Adaptive Optics**. High performance wavefront correction is employed to minimize the intensity of the residual starlight speckle halo.

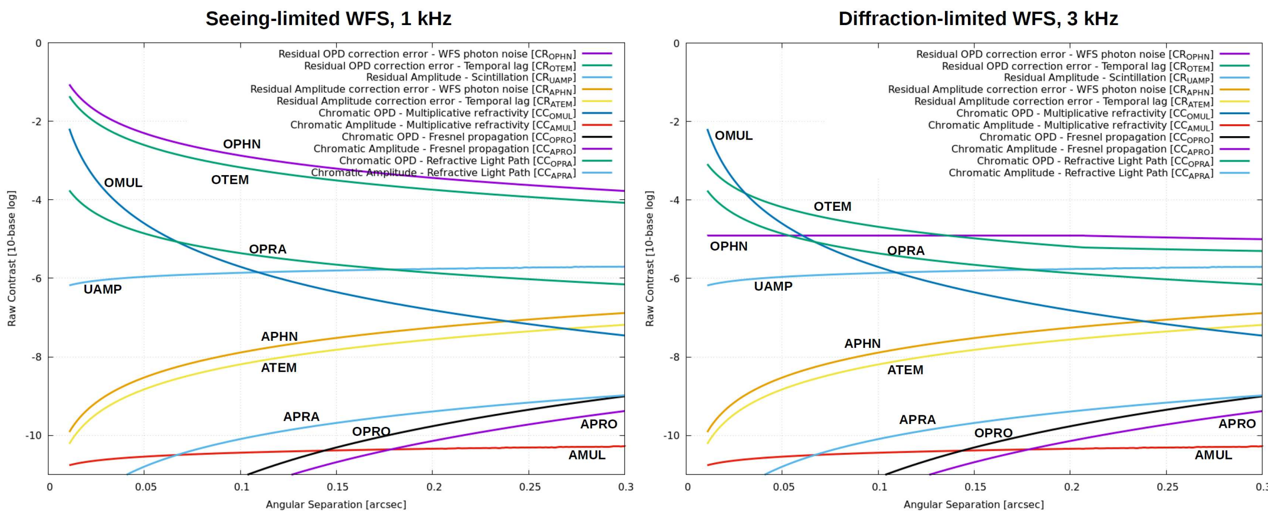

Figure 2. Raw contrast terms for a simulated observation of a M4 star at 5pc with a 30m diameter ground-based telescope. Wavefront sensing is performed in I band, and raw contrast is measured in J band. Curves start at a 1.3 λ/D angular separation corresponding to the coronagraph inner working angle (IWA). The region of interest for habitable planet imaging is within 50mas, at the leftmost part of this figure. Two cases are shown: seeing-limited WFS running at 1 kHz frame rate (left) and diffraction-limited WFS running at 3 kHz frame rate (right).

- **Differential detection techniques** are employed to identify exoplanet light among the residual starlight halo.

We focus, in this publication, on the Extreme Adaptive Optics (ExAO) system. Requirements for the ExAO system were derived and reported in a previous publication.[2] Key finding from this previous work are recalled here, and assumed in this publication:

The optimal wavelength range for reflected light imaging and spectroscopic characterization of potentially habitable planets is near-IR: J band and H band ($\approx$ 1 μm to 1.8 μm). The most favorable targets are mid-M type main sequence stars.

To characterize nearby potentially habitable planets around nearby M-type stars, the ExAO system must deliver $\approx$ 1e-5 raw contrast in J-band. Deeper contrast levels are highly beneficial, as stellar photon noise is the dominant fundamental source of noise.

The optimal primary WFS wavelength for reflected light imaging of habitable planets is I band ($\approx 0.9\mu m$). This is the wavelength for which photon-noise limited wavefront sensing is most sensitive.

2. RAW CONTRAST ERROR BUDGET

We consider observation of a M4-type main sequence star at a 5pc distance, as a representative example for reflected light imaging of habitabe planets around nearby M-type stars. The star apparent magnitudes are $m_I = 9$ and $m_J = 7.3$ in the wavefront sensing and science imaging bands respectively. The reflected light contrast for an Earth-like planet in the habitable zone is C=5e-8 at maximum elongation.

A semi-analytical approach estimating, for each spatial frequency, the contribution of several key error terms, is adopted[3] to establish a raw contrast error budget. Results are shown in Figure 2 for two ExAO designs: a 1 kHz seeing-limited WFS such as the Shack-Hartman WFS (left), and a 3 kHz diffraction-limited WFS operating near the optimal photon-noise limit. Starlight suppression residuals are not considered: contrast residuals are entirely due to wavefront control errors in this simulation. Simulation parameters are listed in table 1. In accordance with findings reported in §1.3, wavefront sensing is performed in I band to maximize sensitivity.

Table 1. Simulation Parameters

	Value	Notes
Star brightness, I band	$m_I = 9$	M4 star at 5pc
Star brightness, J band	$m_J = 7.3$	M4 star at 5pc
WFS wavelength	797 nm	Central wavelength
WFS bandwidth	$d\lambda/\lambda = 0.2$	
WFS photometric efficiency	0.2	Overall quantum efficiency
WFS optical sensitivity	$\beta = \sqrt{2}$	for diffraction-limited WFS
AO loop latency	2 frames	2 ms at 1 kHz
Fried Parameter	0.15m	at $\lambda = 550nm$
Wind speed	10 m/s	
Turbulence layers	6	from ground to 16 km
Site Elevation	4200 m	
Zenith angle	40 deg	
Control law	integrator	optimal Fourier gain

Eleven error terms are quantified as part of the analysis. The first 5 are achromatic residuals due to limitations of the ExAO correction:

- **[OPHN] Optical Pathlength Difference (OPD) error due to WFS photon noise**.
- **[OTEM] OPD error due to AO temporal lag**. The WFS Photon noise and time lag [OPHN and OTEM] terms are fundamentally linked: their amplitude is driven by a tradeoff between incoming starlight flux and control loop speed. The ExAO WFS frame rate and gain should be optimally chosen to minimize the sum of the two terms.
- **[UAMP] Scintillation**: As light propagates through the turbulent atmosphere, phase errors are partially converted into amplitude modulation.
- **[APHN] Amplitude measurement due to WFS photon noise**
- **[ATEM] Amplitude measurement temporal lag**

Chromatic terms due to the difference in wavelength between the wavefront sensing and high contrast imaging paths are also derived:

- **[OMUL] Chromatic OPD due to differential multiplicative refractivity**. The refractive index of air is chromatic, so there is multiplicative factor in optical path length (OPD) between the WFS wavelength and the high contrast imaging wavelength.
- **[AMUL] Chromatic OPD due to differential multiplicative refractivity**
- **[OPRO] Chromatic OPD due to differential Fresnel propagation**
- **[APRO] Chromatic amplitude due to differential Fresnel propagation**
- **[OPRA] Chromatic OPD due to differential refractive light path**. The light path from the target to the telescope is chromatic due to atmospheric refraction, creating a chromatic shear term between the WFS and imaging wavelengths.

- **[APRA] Chromatic amplitude due to differential refractive light path**

We first consider an ExAO loop based on a seeing-limited WFS such as a Shack-Hartmann sensor with a 1kHz frame rate (left panel). The analysis reveals that the dominant error terms, OPHN and OTEM, are fundamentally due to lack of sensitivity in the WFS measurement, contributing to a $\approx$ 1e-2 raw contrast level within 50mas of the optical axis (three orders of magnitude larger than the 1e-5 required raw contrast). Other terms are much smaller.

A more sensitive WFS, operating in the diffraction-limited regime (for example a pyramid WFS), along with a higher frame rate, significantly reduces the OTEM and OPHN terms (right panel). The total contrast at 50mas separation is then $\approx$ 1e-4, about one order of magnitude from the requirement. To further improve contrast, the following terms must be addressed:

- WFS sensitivity and temporal lag must be further optimized.
- Chromaticity must be addressed.
- Scintillation must also be addressed to reach 1e-6 raw contrast.

The ExAO system wavefront control architecture discussed in the next section addresses these terms.

3. WAVEFRONT CONTROL ARCHITECTURE

The main fundamental challenges to ExAO wavefront control are **sensitivity**, **temporal response** and **chromaticity**, as described in §2. Additionally, high contrast imaging systems must finely control non-common path errors to ensure that the wavefront at the coronagraph entrance is zero-mean. Finally, fine calibration of residual wavefront errors is critical for detection of sources (planets) well below the raw contrast level.

Technical solutions to meet these challenges have been identified and are under active development:

- **Sensor Fusion and Predictive Control** can simultaneously increase the ExAO system sensitivity and eliminate temporal lag error. Data from multiple sensors can be merged to improve the photometric sensitivity and reduce measurement null space. Predictive control also allows more sensitive WFS measurements,[4,5] and replaces temporal lag by a much smaller extrapolation error. The two techniques are key to reducing the OTEM and OPHN terms
- In **Speckle control**, the complex amplitude of speckles is measured in the focal plane[6,7] to drive a control loop optimize for coherent nulling of residual starlight. IF deployed at, or near the high contrast imaging wavelength, the technique addresses chromatic error budget terms, including OMUL and OPRA. Speckle control naturally addresses non-common path errors. A fast sensitive focal plane nearIR detector, such as MKIDs[8] or SAPHIRA,[9] is needed to temporally resolve fast-changing atmospheric speckles.
- **PSF reconstruction** can be performed from AO system telemetry, provided that a sufficiently accurate calibration can be derived or measured.

3.1 Notional system Architecture

Figure 3 describes how the techniques may be integrated together in a full ExAO system for an ELT.

A first stage AO loop reduces the total wavefront error so that the first stage WFS can operate in the highly efficient diffraction-limited regime. This first stage delivers to the rest of the ExAO system a well-corrected beam free of large wavefront excursions, allowing for high-sensitivity WFS options to be used downstream.

The second-stage ExAO loop performs fine control requiring exquisite precision and calibration. This fine correction may rely of three types of sensors:

- High precision pupil-plane WFS(s)

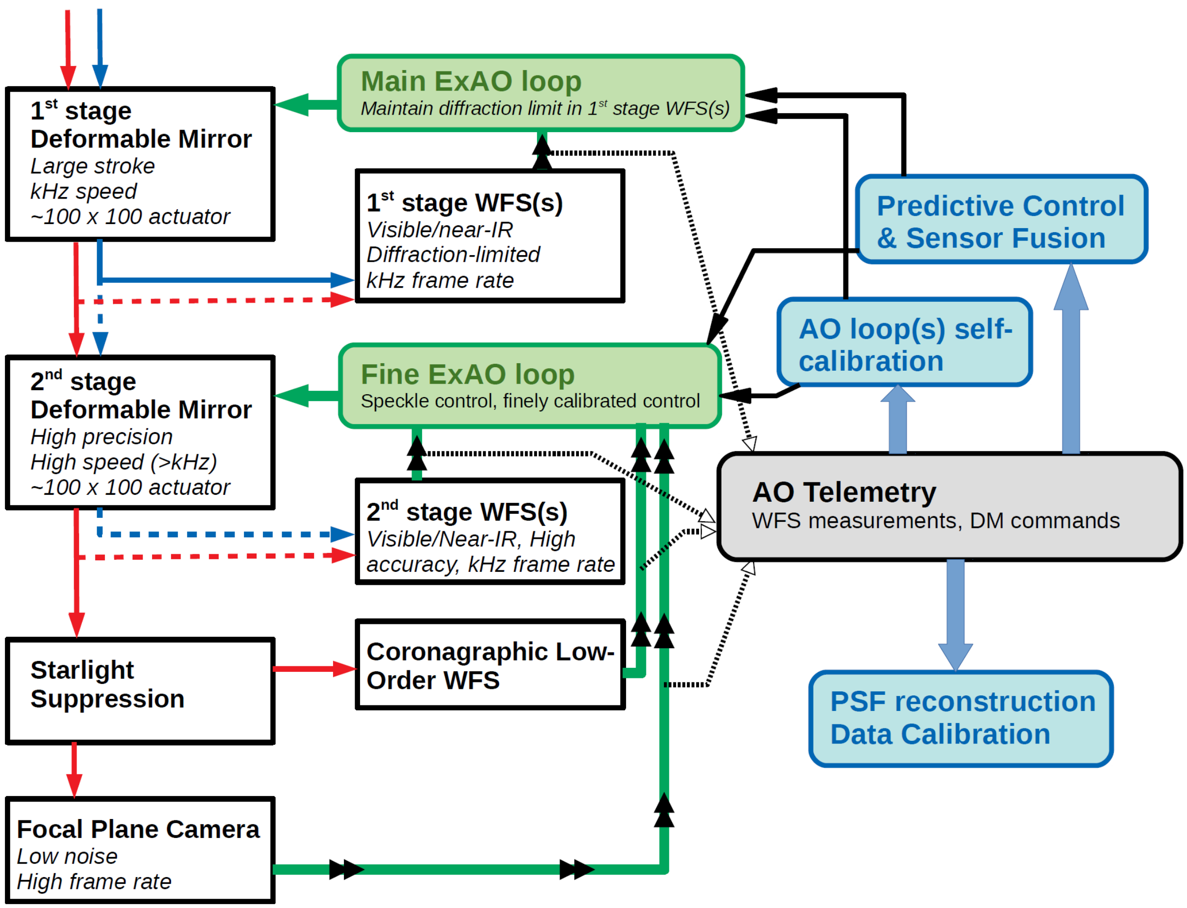

Figure 3. Conceptual ExAO wavefront control architecture optimized for high contrast imaging on ELTs.

- A coronagraphic low-order WFS, capturing near-IR starlight that is rejected by the coronagraph to lock the fine alignment that is critical to starlight suppression. The sensor measures tip-tilt and a few other low-order modes.
- Focal plane WFS, such as specke nulling, or Linear Dark Field Control (LDFC). The loop operates from focal plane image(s) to track and suppress speckles in real time. The loop ensures that no static or slow speckle is left in the image, and provides absolute measurement of residual starlight for post-processing.

4. TECHNOLOGY VALIDATION

Technology validation for ExAO on ELTs relies on a combination of laboratory and on-sky validation efforts. We describe in this section how the Subaru Coronagraphic Extreme-AO (SCExAO) system is providing the hardware platform and software infrastructure for on-sky validation of the ExAO systems envisioned for ELTs. Parallel development programs relevant to ExAO for ELTs include Keck/KPIC,[10] and Magellan/MagAO-X.[11]

The Subaru Coronagraphic Extreme AO (SCExAO) platform, shown in Figure 4, implements much of the conceptual ExAO architecture shown in Figure 3, combining wavefront control and starlight suppression. SCExAO is both a nighttime science instrument and a development platform for high contrast imaging. Much of the system can be tested off-sky with an internal broadband calibration source. SCExAO is optimized to facilitate the development path from concept to on-sky deployment. The large set of high-speed cameras, instruments and dedicated WFSs on SCExAO is of particular interest for validation of advanced WFS/C techniques and approaches.

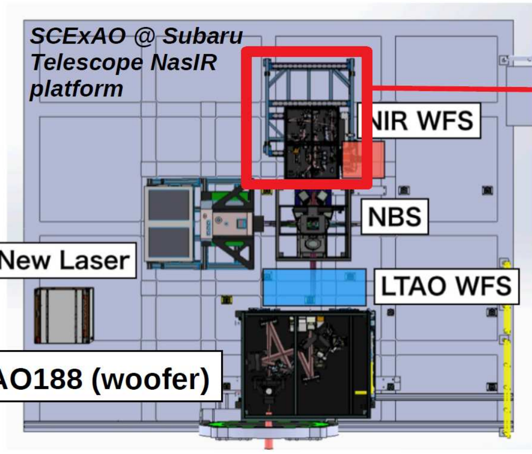

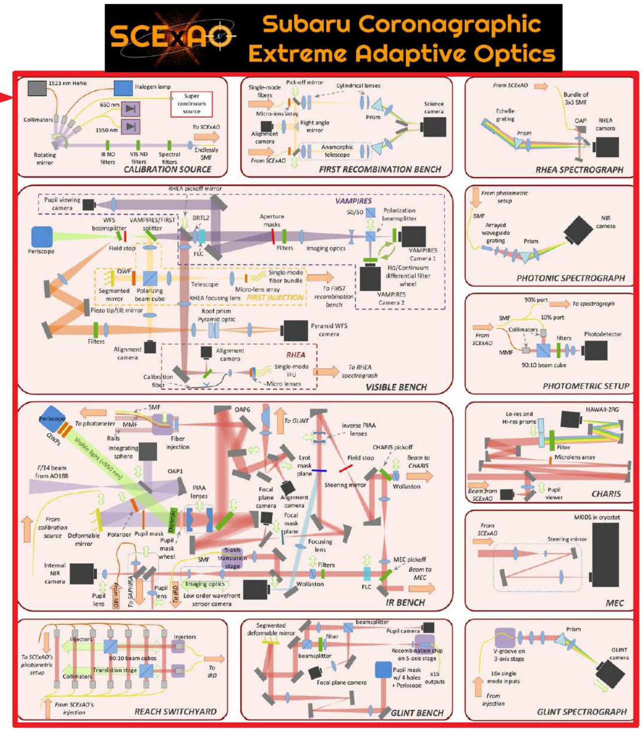

Wavefront Sensors & high speed Cameras				Status
Curvature	VIS (400-600nm)	2 kHz	188 APDs	In operation
SHWFS x4	VIS	~kHz	25x25 cells, sCMOS	2021
Pyramid	600nm-900nm	3.5 kHz	120x120 EMCCD	In operation
LOWFS	0.9-1.7um	<6 kHz	CRED2 InGaAs	In operation
MEC (FPWFS)	0.9-1.4 um	2 kHz	MKIDS photon counting	In operation
VAMPIRES (FPWFS)	0.6-0.8 um	~1 kHz	512x512 EMCCD (x2)	In operation
NearIR pyram	0.9-1.8 um	3 kHz	MCT array (CRED1)	Early 2020
GLINT interferometer	0.9-1.7 um	1.4 kHz	InGaAs (CRED2)	In operation

Figure 4. SCExAO Architecture. Top right: Telescope platform hosting the adaptive optics instrumentation, including SCExAO. Right: Optical path inside the SCExAO system, featuring multiple WFS. Bottom left: List of WFSs and high speed cameras.

On-sky deployment of advanced WFS/C approaches requires software integration between the deformable mirror(s), camera(s) and WFS(s) in a real-time control environment. The Compute and Control for Adaptive Optics (CACAO), co-developed by several AO experts and software engineers, is aimed at providing an open-source software platform solution combining flexibility, high performance and modularity for easy development and validation of advanced WFS/C approaches. Its central feature, shared by ExAO systems at Subaru, Magellan, and Keck, is a common data format allowing fast I/O with multiple processes.

ACKNOWLEDGMENTS

The author acknowledges funding support from the Japanese Society for the Promotion of Sciences (JSPS grants #23340051, #26220704, #23103002, #19H00703 and #19H00695), the Astrobiology Center of the National Institutes for Natural Sciences, Japan, the Mt Cuba Foundation and the directors contingency fund at Subaru Telescope.

REFERENCES

[1] C. Marois, "Thermal Imaging of Earth-size temperate planets orbiting neighborhood stars," *Proc. SPIE* **10702**(154), 2018.

[2] O. Guyon, B. Mazin, M. Fitzgerald, D. Mawet, C. Marois, A. Skemer, J. Lozi, and J. Males, "Wavefront control architecture and expected performance for the TMT Planetary Systems Imager," in *Proc. SPIE*, *Society of Photo-Optical Instrumentation Engineers (SPIE) Conference Series* **10703**, p. 107030Z, Jul 2018.

[3] O. Guyon, "Limits of Adaptive Optics for High-Contrast Imaging," *ApJ* **629**, pp. 592–614, Aug. 2005.

[4] O. Guyon and J. Males, "Adaptive Optics Predictive Control with Empirical Orthogonal Functions (EOFs)," *ArXiv e-prints* , July 2017.

[5] J. R. Males and O. Guyon, "Ground-based adaptive optics coronagraphic performance under closed-loop predictive control," *Journal of Astronomical Telescopes, Instruments, and Systems* **4**, p. 019001, Jan. 2018.

[6] F. Martinache, O. Guyon, N. Jovanovic, C. Clergeon, G. Singh, T. Kudo, T. Currie, C. Thalmann, M. McElwain, and M. Tamura, "On-Sky Speckle Nulling Demonstration at Small Angular Separation with SCExAO," *PASP* **126**, p. 565, June 2014.

[7] M. Bottom, J. K. Wallace, R. D. Bartos, J. C. Shelton, and E. Serabyn, "Speckle suppression and companion detection using coherent differential imaging," *MNRAS* **464**, pp. 2937–2951, Jan. 2017.

[8] S. R. Meeker, B. A. Mazin, R. Jensen-Clem, A. B. Walter, P. Szypryt, M. J. Strader, and C. Bockstiegel, "Design and Development Status of MKID Integral Field Spectrographs for High Contrast Imaging," in *Adaptive Optics for Extremely Large Telescopes IV (AO4ELT4)*, p. E75, Dec. 2015.

[9] D. E. Atkinson, D. N. B. Hall, I. M. Baker, S. B. Goebel, S. M. Jacobson, C. Lockhart, and E. A. Warmbier, "Next-generation performance of SAPHIRA HgCdTe APDs," in *High Energy, Optical, and Infrared Detectors for Astronomy VII*, *Proc. SPIE* **9915**, p. 99150N, Aug. 2016.

[10] N. Jovanovic, J. R. Delorme, C. Z. Bond, S. Cetre, D. Mawet, D. Echeverri, J. K. Wallace, R. Bartos, S. Lilley, S. Ragland, G. Ruane, P. Wizinowich, M. Chun, J. Wang, J. Wang, M. Fitzgerald, K. Matthews, J. Pezzato, B. Calvin, M. Millar-Blanchaer, E. C. Martin, E. Wetherell, E. Wang, S. Jacobson, E. Warmbier, C. Lockhart, D. Hall, R. Jensen-Clem, and E. McEwen, "The Keck Planet Imager and Characterizer: Demonstrating advanced exoplanet characterization techniques for future extremely large telescopes," *arXiv e-prints* , p. arXiv:1909.04541, Sep 2019.

[11] L. M. Close, J. R. Males, O. Durney, C. Sauve, M. Kautz, A. Hedglen, L. Schatz, J. Lumbres, K. Miller, K. Van Gorkom, M. Jean, and V. Gasho, "Optical and mechanical design of the extreme AO coronagraphic instrument MagAO-X," in *Proc. SPIE*, *Society of Photo-Optical Instrumentation Engineers (SPIE) Conference Series* **10703**, p. 107034Y, Jul 2018.